Jour. Korean Inst. Mining Geol.
Vol. 25, No. 3, p. 233-243. 1992.

Genetic Environments of Hydrothermal Copper Deposits in Ogsan Mineralized Area, Gyeongsangbukdo Province*

Seon-Gyu Choi**, Sang-Hoon Choi**, Seong-Taek Yun**,
Jae-Ho Lee** and Chil-Sup So**

ABSTRACT: Ore mineralization of the Hwanghak copper deposit in the Ogsan area occurred in three stages of quartz (stage I and II) and calcite (stage III) veining along fissures in Early Cretaceous sedimentary rocks. Ore minerals are pyrite, pyrrhotite, chalcopyrite (dominant), sphalerite, hematite, galena, and Ag-, Pb-, and Bi-sulfosalts. These were deposited during the first stage at temperatures between 370° and <200℃ from fluids with salinities between 0.5 and 7.6 equiv. wt. % NaCl. There is evidence of boiling and this suggests pressures of less than 180 bars during the first stage. Equilibrium thermodynamic interpretation accompanying with mineral paragenesis and fluid inclusion data indicates that copper precipitation in the hydrothermal system occurred due to cooling and changing in chemical conditions (fs_2, fo_2, pH). Gradual temperature decrease from 350° to 250℃ of ore fluids by boiling and mixing with less-evolved meteoric waters mainly led to copper deposition through destabilization of copper chloride complexes.

Sulfur isotope values of sulfide minerals decrease systematically with paragenetic time from calculated $\delta^{34}S_{H_2S}$ values of 8.2 to 4.7‰. These values, together with the observed change from sulfide-only to sulfide-hematite assemblages and fluid inclusion data, suggest progressively more oxidizing conditions, with a corresponding increase of the sulfate/H_2S ratio of hydrothermal fluids. Measured and calculated hydrogen and oxygen isotope values of ore-forming fluids suggest meteoric water dominance, approaching unexchanged meteoric water values.

INTRODUCTION

The Cu-bearing hydrothermal vein-type deposits occur within Cretaceous volcanic and sedimentary rocks in the Gyeongsang Basin of the southern Korean peninsula. Most Cu-bearing veins occur in three areas (Goseong, Haman-Gunbuk, and Euiseong) where they are associated with Cretaceous granites (Sillitoe, 1980, Jin et al., 1982, Park et al., 1985 and So et al., 1985). It is known that Korean Cu-bearing hydrothermal ore deposits display similarities in mineralogy, temperatures, salinities, pressure, and mineralization age. Fluid inclusion and stable isotope studies suggest that ore deposition in the Goseong Cu mineralization area was likely a result of increasing influx of meteoric waters in hydrothermal system (So et al., 1985).

The Hwanghak mine in the Ogsan area is located approximately 7 km northeast of Euiseong. The regional geological survey of the area was carried out by Chang et al. (1978) but the ore mineralogy, and physical and chemical conditions at ore deposition have not been documented. In this paper, we document the physical and chemical conditions of ore mineralization of the Hwanghak copper deposit in the Ogsan area.

* This paper was supported by NONDIRECTED RESEARCH FUND, Korea Research Foundaton, 1991.

** Department of Geology, Korea University, 1, Anam-dong, Seongbuk-ku, Seoul 136-701, Korea.

GEOLOGY

The Hwanghak mine is located approximately 200 km southeast of Seoul in the northwestern part of the Gyeongsang Basin. The sedimentary rocks are intruded by late Cretaceous (Bulgugsa) igneous rocks. Cu(+Pb+Zn)-bearing quartz veins cut Cretaceous sedimentary rocks (Fig. 1).

A Jurassic biotite-hornblende granite (Cheongsong Granite) in the northeast of the area, is unconformably overlain by the Ilchik Formation of the Hayang Group (Gyeongsang Supergroup). The granite is composed mainly of quartz, plagioclase, microcline, biotite, hornblende and minor amounts of sphene, muscovite, apatite, and zircon. The Hayang Group (<5,000 m thick) is composed mostly of shale, sandstone (and a minor amounts of marl), and locally derived conglomerate (Lee, 1987). In the Hwanghak mine, the Hayang Group succession is,

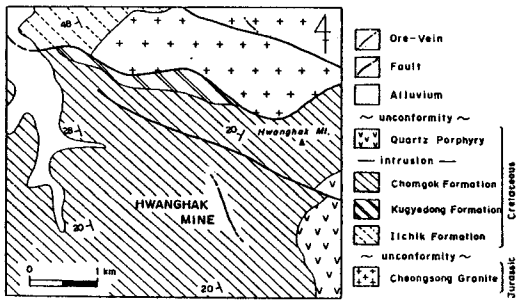

Fig. 1. Geologic map of the Hwanghak Cu mine area.

in ascending order, the Ilchik, Kugyedong and Chomgok formations (Fig. 1).

The Ilchik and Kugyedong formations crop out in a limited area in the nothern part of the mine area. The Ilchik Formation, ≤800 m thick, is composed basal conglomerate, pebble-bearing sandstone, shale, and green sandstone. The Kugyedong Formation, ≤400 m thick, is composed of 10 layers of red shale interstratified with red sandstone.

The Chomgok Formation, 950 m thick, strikes N10° to 45°W, dip 15° to 35°SW and is composed mainly of alternations of gray to greenish grey fluvio-lacustrine sandstone and shale interlayered with minor conglomerate and green tuff (Chang et al., 1978). It conformably overlies the Kugyedong Formation and is intruded by late Cretaceous quartz porphyry in the southeast of the area (Fig. 1).

ORE VEINS

Hwanghak deposit is composed of polymetallic, Cu (-Pb-Zn) bearing hydrothermal quartz and calcite veins crosscutting older sedimentary rocks of the Cretaceous Chomgok Formation. The economically viable quartz vein generally has about 10 cm to 50 cm thick. Numerous thinner veins occur parallel to the principal vein through with abundant splits. The vein shows slight variations of strike and dip. The general trend is N10°W to N20°W with dips of 80° to 90°SW. It is composed chiefly of quartz, fluorite and calcite, with chalcopyrite, sphalerite and galena as the dominant ore minerals. Outward from the vein margins, the changes of hydrothermal alteration mineral which may be related to from the early to late vein mineralization are shown with following predominant mineral sequence: kaolinite; sericite; and chlorite.

Cu-bearing hydrothermal veins are tabular, coarse grained massive and often contain brecciated host

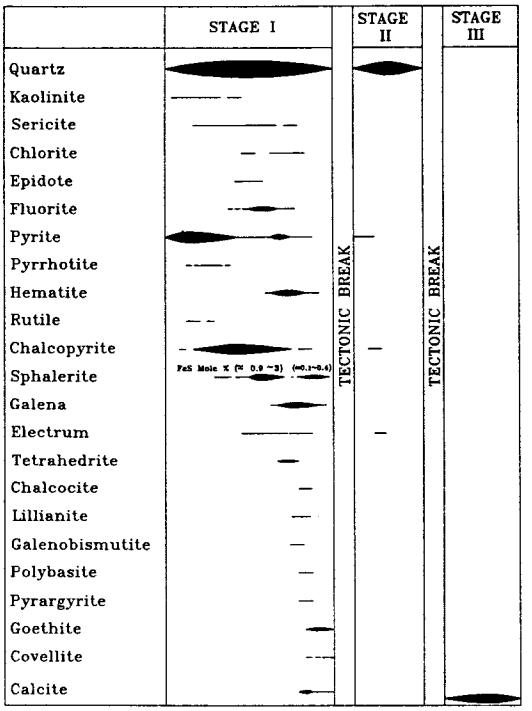

Fig. 2. Generalized paragenetic sequence of minerals from veins of the Hwanghak Cu mine. Width of lines corresponds to relative abundance.

-rock fragments (<5 cm across). Small vugs are common. They contain milky to clear euhedral quartz commonly associated with calcite and late ore minerals. Most contacts between host-rock and veins are sharp. Within ore shoots, sulfide-rich zones of coarse-grained chalcopyrite, sphalerite and galena occur in intermediate portion of veins, whereas disseminated fine grains occur in central portions. Lateral mineral zoning of the veins are common, with a mineral sequence from the vein margin to center: pyrite+pyrrhotite; pyrite+chalcopyrite+dark-brown sphalerite; and yellowish-brown sphalerite+galena.

MINERALOGY AND PARAGENESIS

Massive, banded and brecciated and mixed ores characterize the mine. Textural relationships indicate that the veins were formed in three stages separated by tectonic fracturing and brecciation events (Fig. 2). During stage I, milky to clear quartz and fluorite with economic concentrations of Cu, base-metal sulfides and rare sulfosalts were deposited. In stage

II, barren massive white quartz with minor amounts of base-metal sulfides were introduced into the fault vein system. Stage III deposited barren calcite. All three stages are displayed together only in the principal vein of the Hwanghak mine.

Stage I Mineralization

Stage I veins contain all of the economic mineralization. Milky to clear quartz is the most abundant mineral and mainly occurs as massive. Clear, euhedral quartz crystals (up to 0.3 cm long) are frequently found in vugs. Medium sized grains of fluorite occur locally near vein margins. Chlorite is associated with ore minerals along vein margins and intermediate zones of the vein, and it also occurs disseminated throughout the veins.

Primary ore minerals of stage I are pyrite, pyrrhotite, rutile, chalcopyrite, sphalerite, hematite, galena, tetrahedrite, chalcocite, Pb-Bi-sulphosalts, electrum, and Ag-sulphosalts. Products of early stage I mineralization are characterized by the pyrite +pyrrhotite; main mineralization is characterized by chalcopyrite+sphalerite+galena and hematite; and late mineralization is characterized by galena+Pb-Bi-sulphosalts+Ag-sulphosalts. These minerals occur as intergranular crystals and massive aggregates within quartz. Late yellowish brown sphalerite commonly overgrow clear quartz in vugs or occurs near vugs.

Pyrite, one of the dominant sulfides, is ubiquitous as fine to coarse crystalline aggregates. It occurs mainly as subhedral to euhedral disseminated grains and locally is concentrated in massive veinlets (up to 0.3 cm) near vein margins and in fractures in wall-rock. Fine euhedral grains common disseminated in the wall-rocks. Highly brecciated fragments of early pyrite are commonly cemented by chalcopyrite. Pyrrhotite often occurs as inclusions in early subhedral pyrite.

Chalcopyrite, the most dominant copper mineral in the mine, mainly occurs as masses with an irregular outline and as medium to fine-grained disseminates. It also occurs as anhedral grains intergrown with other sulfides. Chalcopyrite was associated with pyrite in the early period of stage I, with galena-sphalerite in the base metal sulfide assemblage and with Pb-Bi- and Ag-Sb-sulfosalts during the late period of stage I mineralization, indicating that chalcopyrite was deposited over a long period.

Two types of sphalerite are widely distributed and formed at different times. The sphalerite occurs: 1) as common polycrystalline aggregates associated with chalcopyrite in the intermediate zone of the veins (early sphalerite), 2) as medium grained disseminates near vugs, or associated with galena and sulphosalts (late sphalerite). These two types of sphalerite are also distinguished by color (1) dark brown, 2) yellowish brown) and Fe contents (1) 0.9~3 mole% FeS, 2) 0.1~0.4 mole% FeS). Highly brecciated early sphalerite is cemented and replaced by galena and tetrahedrite. Chalcopyrite inclusions in early sphalerite are common, but in late yellowish brown sphalerite they are rare or absent. Coarse-grained galena occurs as anhedral grains and disseminated in the intermediate zone (rarely near vugs) of the veins. It is commonly interstitial to sphalerite and chalcopyrite. Fine irregular electrum occurs with sphalerite and/or galena. It contains ≈ 52 to ≈ 41 atomic percent silver.

Euhedral hematite tabular crystals and laths are common, and hematite mainly occurs as fibrous or radiated aggregates of needle-shaped crystal and is interstitial to euhedral quartz crystals. It shows transverse micro-scale twinning. Minor amounts of hematite are disseminated in the marginal portions of stage I quartz veins. Rutile rarely occurs as inclusion in hematite.

Tetrahedrite is commonly associated with galena. Anhedral tetrahedrite is often interstitial between sphalerite and galena margins and rarely co-precipitated with Pb-Bi sulphosalts within galena. Sulphosalt mineralization occurred in the late period of stage I. This mineralization is represented by Cu-Ag-Sb (tetrahedrite), Pb-Bi (lillianite and galenobismutite) and Ag-Sb (polybasite and pyrargyrite), sulphosalts with galena and minor amounts of base metal sulfides. Rounded or irregular grains of sulphosalt minerals in galena are interstitial to other sulfides or euhedral quartz crystals near vugs. Goethite and covellite occur as alteration products. Goethite replaced mainly hematite and galena. Covellite mainly replaced along grain margins of chalcopyrite.

Stage II Mineralization

Stage II veins are composed of white quartz and minor amounts of pyrite, chalcopyrite and galena and occurs as irregularly-oriented barren quartz veinlets (maximum thickness of 5 cm, and usually less than 1 cm in thickness) crosscutting stage I quartz veins. Fine-grained ore grains disseminate throughout the

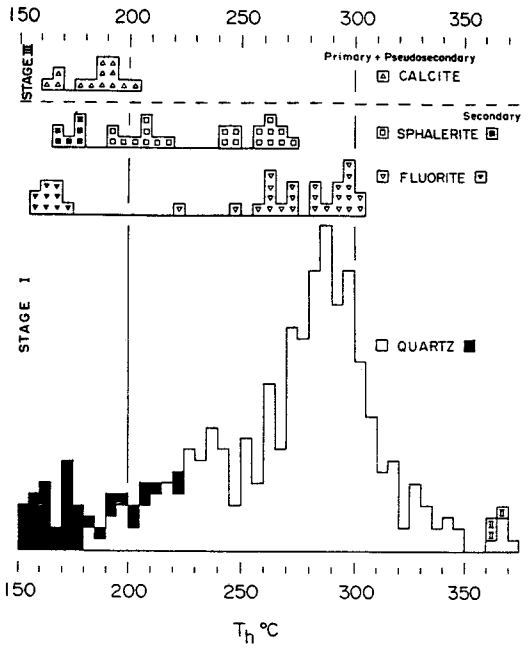

Fig. 3. Frequency histograms of fluid inclusion homogenization temperatures in vein minerals of the Hwanghak Cu mine. II=type II inclusions.

stage II vein.

Stage III Mineralization

Barren milky white calcite veins were formed during this stage, which is the final hydrothermal stage. The latest phase of tectonic activity occurred often mineralization of the stage II veins. These veins often crosscut earlier veins.

FLUID INCLUSION STUDIES

Fluid inclusions (over 380 primary and pseudosecondary, over 50 secondary) were examined in 48 samples of quartz, fluorite, sphalerite and calcite from the Hwanghak mine using a Leitz microscope equipped with a FLUID Inc. heating-freezing stages. Fluid inclusion investigations were undertaken in order to document the ranges of fluid composition and temperatures during the periods of mineralization at Hwanghak mine and to investigate their variations in time. Temperatures of homogenization and ice melting have standard errors of $\pm 1.0°$ and $\pm 0.2℃$, respectively. Salinity data based on freezing point depression in the system H_2O-NaCl (Potter et al., 1978). The result of heating and freezing experiments of fluid inclusions are presented in Figs. 3 and 4.

Two types of fluid inclusions ranging in size from <3 to >40 μm were observed: liquid-rich type I and rare vapor-rich (or vapor-filled: detected under the microscope) type II. No liquid CO_2-bearing inclusions were observed.

Most inclusions are liquid-rich and contain liquid and a small vapor bubble comprising 10~30% of the total volume of each inclusion at room temperatures. These inclusions do not contain daughter minerals and readily homogenize to the liquid phase. No traces of gas hydrates were observed during freezing.

Vapor-rich inclusions contain a liquid and a vapor bubble comprising >70 volume percent of the inclusion at room temperature. These rare inclusions homogenize to the vapor phase, and only occur as primary inclusions in stage I white to clear quartz. Almost of the vapor-rich inclusions are too small for fluid inclusion study and do not contain daughter minerals.

Inclusions in Stage I Veins

Minerals examined are milky to clear quartz, fluorite and sphalerite. Fluid inclusions in earlist milky quartz contains liquid-rich and vapor-rich fluid inclusions. Inclusions in later quartz, fluorite and sphalerite are dominantly liquid-rich inclusions.

Primary and pseudosecondary inclusions in stage I minerals homogenize from 372° to 182℃. Homogenization temperatures of primary and pseudosecondary liquid-rich and vapor-rich inclusions in quartz are 372° to 182℃ and 369° to 362℃, respectively (Fig. 3). Primary and pseudosecondary, liquid-rich inclusions in fluorite and sphalerite homogenized at temperatures of 302° to 222℃ and 273° to 204℃, respectively.

Early dark-brown to late yellowish-brown vug sphalerite occurs in this deposit (see "Mineralogy and Paragenesis"). Homogenization temperatures of primary liquid-rich inclusions in these sphalerite ranges from early to late, are 273°~242℃ and 218°~204℃, respectively, and indicate a progressive cooling with increasing paragenetic time (Fig. 3).

Salinities of primary and pseudosecondary liquid-rich inclusions in stage I quartz, fluorite and sphalerite are 0.4~7.6, 1.4~4.9 and 0.5~4.2 wt.% equiv. NaCl, respectively (Fig. 4). Those for primary vapor-rich inclusions in quartz ranges from 0.7 to 1.5 wt.% equiv. NaCl. Salinities of primary inclusion in sphalerite also decrease from early dark-brown (4.2~3.4 wt.% equiv. NaCl) to late yellowish-brown

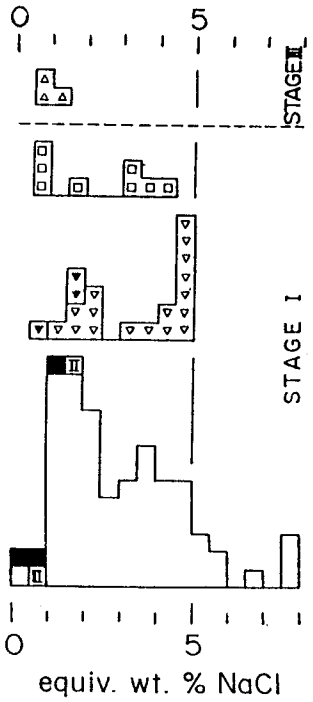

Fig. 4. Frequency histograms of fluid inclusion salinities in vein minerals of the Hwanghak Cu mine. Symbols are the same as in Fig. 3.

vug sphalerite (1.6~0.5 wt.% equiv. NaCl).

Secondary fluid inclusions in stage I minerals are all liquid-rich. They homogenize from about 150° to 220℃ and have salinities between 0.4 and 1.9 wt.% equiv. NaCl (Figs. 3 and 4). These homogenization temperatures are similar to those of primary and pseudosecondary liquid-rich type inclusions in stage III calcite (Fig. 3).

Inclusions in Stage II Veins

Fluid inclusions in massive white quartz of stage II are very rare and too small for fluid inclusion investigation. Therefore, the homogenization temperatures measurements of fluid inclusions are imprecise. They homogenize at temperatures of about 200°~300℃ (peak temperature range about 240°~260℃). These results indicate that the mineralization of stage II vein occur at lower temperatures than the mineralization of stage I vein.

Inclusions in Stage III Veins

Primary fluid inclusions in stage III calcite are all liquid-rich and larger ($\approx 20\,\mu m$) than those of other earlier formed minerals. They homogenize at temperatures of 162°~203℃ (Fig. 3). Salinities of these inclusions range from 0.5 to 1.1 wt.% equiv. NaCl (Fig. 4).

Variations in Temperature and Composition of Hydrothermal Fluids

During mineralization episodes, variations in temperature and composition of the hydrothermal fluids are recorded by fluid inclusions. The homogenization temperatures of primary and pseudosecondary inclusions in stage I and III minerals range from 372° to 162℃ with salinities between 0.4 to 7.6 wt.% equiv. NaCl. Within this wide range of temperatures and salinities, analysis of peak and clusters of data within frequency diagrams (Figs. 3 and 4) has allowed us to decipher individual events which are probably related to specific mineral assemblages (Shelton, 1983).

Homogenization temperatures of primary and pseudosecondary inclusions in stage I minerals form three main clusters (Fig. 3): (1) a high temperature (370° to 320℃) cluster, corresponding to early quartz+pyrite mineralization; (2) a middle temperature (320° to 240℃) cluster, corresponding to main ore-stage quartz-pyrite-chalcopyrite-dark brown sphalerite mineralization; and (3) a lower temperature (240° to 190℃) cluster, from corresponding to late yellowish brown sphalerite-galena mineralization.

These temperature ranges are in good agreement with pyrite- chalcopyrite and sphalerite-galena sulfur isotope temperatures of 314°± 50℃ and 254°± 35℃ and 202°± 30℃ (see "Stable Isotope Studies").

The relationship between homogenization temperatures and salinities of inclusions in stage I quartz veins of the Hwanghak deposit (Fig. 5) indicates a complex history of boiling, cooling, mixing and dilution.

Almost of the vapor-rich inclusions are very tiny for fluid inclusion study, but the inclusions homogenized from 300° to 370℃ and three precise homogenization temperatures are 369°, 363° and 362 ℃ (Figs. 3 and 5). And these fluid inclusions were trapped simultaneously with liquid-rich inclusions to have the same temperature range. These phenomena were supported by microscopic observation. Therefore, during early mineralization, boiling of ore fluids resulted in an inverse relationship (trend a in Fig. 5) between homogenization temperature and

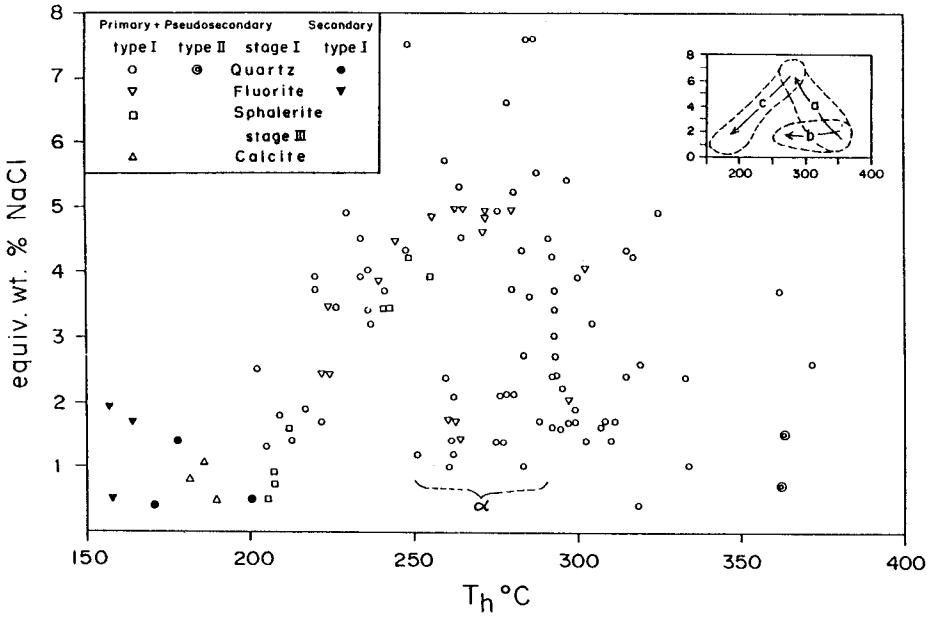

Fig. 5. Homogenization temperature versus salinity diagram for fluid inclusions in stage I and III minerals from Hwanghak Cu mine.

salinities. Boiling of fluids which deposited mainly early quartz in the deposit resulted in an increase in salinity (up to 7.6 wt.% equiv. NaCl) at temperatures near 290℃ (trend a in Fig. 5). The salinity increase reflects concentration of salts in the residual liquid-rich as vapor was lost during boiling. Whilst simple cooling (plus slight dilution by mixing with cooler, less saline fluids) occurred during and after boiling in the residual fluids without boiling effect (trend b in Fig. 5). But another mechanism which produces evolution trend b in Fig. 5 is 'necking-down'. For two-phase (L+V) inclusions, this creates a spread in temperature with no change in salinity (trend b). In the absence of supporting evidence, trends due to simple cooling, leakage and necking are indistinguishable (Shepherd et al., 1985). We are convinced by microscopic evidences that the fluid inclusions in field *α* (Fig. 5) are primary inclusions. During the main part of stage I, boiling of hydrothermal fluids led to high, but variable salinities. Later cooling and dilution of the hydrothermal fluids by mixing with cooler, less saline, less-evolved meteoric waters resulted in the positive linear relationship between temperature and salinities shown in Fig. 5. Fluids ranged from a high temperature, high salinity end-member (by boiling) toward a lower temperature, less saline component (trend c, Fig. 5). By the advent of stage III carbonate deposition, cooling and dilution were more pronounced (temperature, 203° to 162℃; salinity, 0.5 to 1.1 wt.% equiv. NaCl), probably due to repeated fracturing that allowed more dilute meteoric water into the system. These changes would be very likely to resulted in mineral deposition. In particular, economic concentration of Cu mainly occurred in the main portion of changes of physico-chemical conditions : from the early period of boiling (<≈ 310 ℃) to the late period (>≈ 250℃) of cooling and dilution (by mixing).

Boiling and Fluid Pressure

Liquid-rich and vapor-rich inclusions in early stage I quartz from the Hwanghak mine homogenize at the same temperatures over a range from 310° to 360℃. At these temperatures, the wide range of salinity (0.7 to 4.9 wt.% equiv. NaCl) of early stage I ore fluids indicates that boiling occurred throughout early stage I ore deposition (see "Variations in temperature and Composition of Hydrothermal Fluids"). Data for the system H_2O-NaCl (Sourirajan and Kennedy, 1962; Haas, 1971; Cunningham, 1978) combined with the temperature and salinity data for these inclusions, indicate pressures of <180 bars. These pressure correspond to maximum depths of about 700 m and 2400 m, respectively, assuming

lithostatic and hydrostatic loads.

GEOCHEMICAL ENVIRONMENT OF ORE DEPOSITION

Equilibrium thermodynamics are used to estimate the changes in chemical conditions of the hydrothermal fluids during ore and gangue deposition of stage I in the Hwanghak hydrothermal system. Ranges of temperature and fugacity of sulfur (fs_2) for Cu-Pb-Zn mineralization were estimated from phase relations and mineral compositions in the systems Fe-Zn-S (Scott and Barnes, 1971) and Au-Ag-S (Barton and Toulmin, 1964). Fig. 6 indicates a general decrease in fs_2 with time during stage I ore deposition. Pyrite-sphalerite-electrum assemblages (sphalerite: 0.9~3 mole% FeS; electrum: N_{Ag}=0.41~0.52) in the main mineralization of stage I were precipitated within a temperature range of 315° to 230℃, which corresponds to log fs_2 values of −8.5 to −11.5 (Fig. 6). During the later mineralization, sphalerite (0.1 to 0.4 mole% FeS), pyrite, electrum and sulfosalts were deposited with galena and hematite. Maximum temperature and log fs_2 conditions of the later period are defined by the mineral assemblages, above mentioned phase relation and homogenization temperatures of fluid inclusions in the later sphalerite (Fig. 3). The maximum temperature and log fs_2 values are less than 230℃ and ≈ −12.0, respectively.

It is possible to define limits of the fugacities of

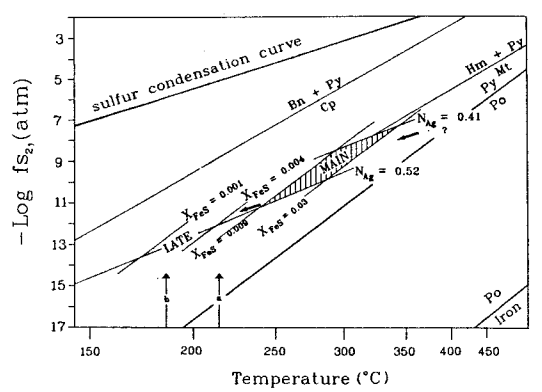

Fig. 6. Fugacity of sulfur versus temperature diagram showing sulfidation reactions. N_{Ag}; atomic fraction of Ag in electrum and X_{FeS}; mole fraction of FeS in sphalerite. "a" and "b" indicate the maximum and minimum homogenization temperature of fluid inclusion in late sphalerite. Arrow represents the evolution trend of decreasing temperature and decreasing fugacity of sulfur in stage I. Abbreviations: Bn; bornite, Cp; chalcopyrite, Hm; hematite, Mt; magnetite, Po; pyrrhotite, and Py; pyrite.

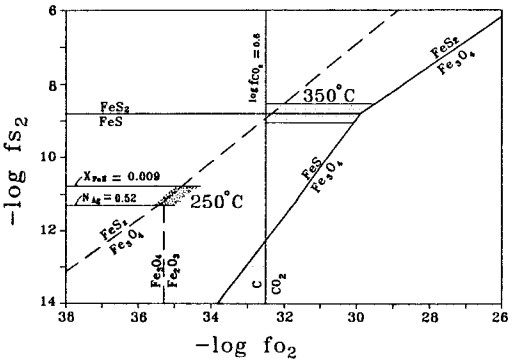

Fig. 7. Fugacity of sulfur versus fugacity of oxygen diagram at 350° and 250℃ showing mineral stabilities at each temperature (dotted areas). Solid lines indicate stability fields of minerals in the system Fe-O-S at 350℃; dashed lines, stability fields of minerals in the system Fe-O-S at 250℃. Equilibrium constants used for constraining reactions are from Helgeson (1969) and Ohomoto (1972).

O_2 and S_2 of the ore fluid in stage I using an fo_2-fs_2 diagram (Fig. 7). Diagrams for fo_2-fs_2 are constructed assuming ore fluid temperatures of 350℃ and 250℃, respectively, for the early and late Cu-mineralization of stage I. For the early mineralization at 350℃, the maximum fo_2 value is defined by the pyrite-pyrrhotite-magnetite reaction because no magnetite is found. The lower fo_2 value is limited by the graphite-CO_2 curve due to the graphite absence. Using Henry's law constant for a 0.9 molar NaCl solution at 350℃ (K=4,300; Ellis and Golding, 1963) and assuming that Xco_2 was less than 0.001 (based on the usual absence of either liquid CO_2 or CO_2 hydrate in fluid inclusion), the probable log fco_2 is estimated to be about 0.63.

The obtained range of log fo_2 at 350℃ is −29.7 to −32.4 (Fig. 7). The common occurrence of pyrite+hematite assemblage in the mineralization at 250℃ can be used to define the fo_2 condition by combining with the compositional range of sphalerite and electrum. Log fs_2 values at 250℃ are −10.6 to −32.5 (Fig. 6). Obtained range of log fo_2 at 250℃ is −34.1 to −35.0 (Fig. 7). The temperature range of Cu mineralization at Hwanghak is estimated 350° ~250℃ by the result of fluid inclusion studies combining with mineral paragenesis. The presence of kaolinite and sericite as a vein-related early alteration mineral (related to the early mineralization) and prevailing presence of sericite as a vein-related alteration mineral (related to the main mineralization) can be used to estimate the pH of hydrothermal fluids at 350℃ and 250℃, respectively.

The pH of the hydrothermal fluids at 350℃ and

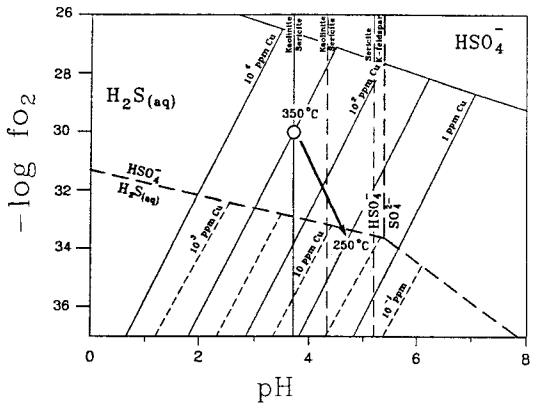

Fig. 8. Solubility of the assemblage pyrite+chalcopyrite (+bornite) in hydrothermal NaCl solution, modified from Crerar and Barnes (1976). Solid and dashed contours indicate the Cu concentration of chloride complex at 350℃ and 250℃, respectively.

250℃ in Hwanghak was controlled by the kaolinite-sericite and sericite-quartz-K feldspar reaction curve. The activity of K^+ was estimated using the temperature dependence of Na/K ratios for natural waters (Fournier and Truesdell, 1973) combined with the salinity (0.9 molar NaCl) of the fluid and the activity coefficients of K^+ (Ohmoto, 1972). The average pH value of the fluids at 350℃ which is therefore set by the mutual stability of kaolinite and sericite is about 3.6. The pH range of the fluids at 250℃ defined by the sericite stability is 4.3 to 5.3. The changes in chemical conditions (temperature, fs_2, fo_2, pH, etc.) of the hydrothermal fluids during stage I mineralization are used to estimate the Cu solubility.

Utilizing solubility data from Crerar and Barnes (1976) for chloride complexing, contours of copper solubility in solution have been plotted in Fig. 8. Fig. 8 shows the pH versus log fo_2 relation at variable copper concentration (ppm). During the early mineralization at 350℃, average pH=3.6 and -log fo_2 range=29.7~32.4, significant amounts of copper (10^3 to 10^2 ppm) could be dissolved in weakly acid NaCl solutions. For the late mineralization at 250℃, pH=4.3~5.3 and -log fo_2=34.1~35, about 10^0 ppm copper could be dissolved. From Fig. 8, the concentration exceeding 10^3 ppm of copper could be dissolved and transported by chloride complex in such solutions. The chemical changes of ore fluids by cooling of the solutions to 250℃ precipitated almost all of the dissolved copper. Available data on copper sulfide solubilities were summarized by Romberger and Barnes (1970), Crerar (1974) and Crerar and Barnes (1976). By these data, the solubility of copper-sulfide complexes is negligible in the solutions, indicating that the sulfides were not effective transporting ligands of Cu in the ore fluids of the Hwanghak deposit.

Copper deposition in the Hwanghak hydrothermal system was likely a result of a progressively decreasing temperature, and the changes in chemical conditions (fs_2, fo_2, pH, etc.) resulting in decrease of solubility of copper chloride complexes. The main precipitation temperatures of copper minerals (estimated by fluid inclusion studies accompaning mineral paragenesis), ≈310℃ to ≈250℃, indicate that cooling (by boiling and mixing, see "Fluid Inclusion Studies") is prominent in the copper mineralization.

STABLE ISOTOPE STUDIES

Table 1. Sulfur isotope data for stage I minerals from the Hwanghak mine.

Sample no.	Mineral	$\delta^{34}S$(‰)	$\Delta^{34}S$(‰)	T(℃)[1]	T(℃)[2]	$\delta^{34}S_{H_2S}$(‰)	Remarks
HW-9	pyrite	9.2			350	8.2	Early
HW-10	pyrite	8.9			350	7.8	Early
HW-12-1	pyrite	9.1	1.3	314± 50	314	7.9	Main
HW-12-2	chalcopyrite	7.8			314	7.9	Main
HW-17-1	sphalerite	6.9	2.6	254± 35	254	6.5	Main
HW-17-2	galena	4.3			254	6.5	Main
HW-2	sphalerite	6.2			270	5.9	Main
HW-14	chalcopyrite	5.8			280	6.0	Main
HW-13	sphalerite	6.1			250	5.6	Main
HW-7-2	sphalerite	5.6	3.2	202± 30	202	5.2	Late
HW-7-1	galena	2.4			202	5.2	Late
HW-1	sphalerite	5.0			210	4.6	Late

[1]: Using the isotope fractionation equations in Ohmoto and Rye (1979). [2]: Based on fluid inclusions and temperatures and paragenetic constraints and/or sulfur isotope temperatures.

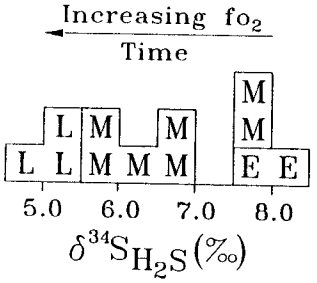

Fig. 9. Sulfur isotope compositions of H_2S in euqilibrium with stage I vein sulfides from the Hwanghak mine. Abbreviations: E; early, M; main, and L; late.

Recent studies have shown the use of stable isotopes in elucidating the origin and history of hydrothermal fluids that formed veins (Taylor, 1973; O'Neil and Silberman, 1974; So et al., 1985). In this study we measured sulfur isotope compositions of sulfide minerals, oxygen isotope compositions of quartz and hydrogen isotope compositions of inclusion waters. Standard techniques of extraction and analysis were used, as described by Grinenko (1962) and Hall and Friedman (1963). Data are reported in standard δ notation relative to the Canon Diablo Troilite (CDT) standard for S and Vienna SMOW for O and H. The analytical error of each analysis is approximately ± 0.1‰ for O and S and ± 1‰ for H.

Sulfur Isotope Study

Twelve stage I sulfide minerals of the Hwanghak mine were analyzed for sulfur isotopes (Table 1). Pyrite-chalcopyrite and sphalerite-galena pairs with equilibrium textures developed during the main mineralization period have $\delta^{34}S$ values of 1.3 and 2.6 ‰, yielding equilibrium isotope temperatures of 314° $\pm$ 50℃ and 254° $\pm$ 35℃ (Ohmoto and Rye, 1979). The late sphalerite-galena pair with equilibrium textures has $\delta^{34}S$ values of 3.2‰, yielding equilibrium isotope temperature of 202° $\pm$ 30℃. These calculated temperatures are in agreement with the range of the homogenization temperatures of primary and pseudosecondary fluid inclusions in sphalerite and associated quartz and fluorite.

Assuming depositional temperatures of $\approx$ 370° to $\approx$ 330℃ for early pyrite, $\approx$ 320° to $\approx$ 230℃ for sulfides of main mineralization period and $\approx$ 220° to $\approx$ 190℃ for late sulfides (based on fluid inclusions, paragenetic constraints, and/or sulfur isotope temperatures), $\delta^{34}S_{H_2S}$ values of hydrothermal fluids were calculated for the sulfide minerals (Ohmoto and Rye, 1979): 8.2 and 7.8‰ (early pyrite); 7.9‰ (pyrite); 7.9 and 6.0‰ (chalcopyrite): 6.5 to 5.6‰ (sphalerite); 6.5‰ (galena); 5.2 to 4.7‰ (late sulfides) (Table 1). Sulfur isotope compositions of H_2S appear to decrease systematically with paragenetic time during stage I (8.2 to 4.7‰) (Fig. 9). Furthermore, the $\delta^{34}S_{H_2S}$ values between the main mineralization period and late period tend to decrease with their detailed paragenetic time (these mineralization periods show mixing with cooler, less saline, less-evolved meteoric waters coupled boiling; see "Variation in Temperature and Composition of Hydrothermal Fluids"). Two possible explanations for this phenomenon are: (1) gradual addition of sulfur from an isotopically light source, or (2) increase in the SO_4/H_2S ratio (by progressive oxidation of the fluid) of the fluid with time. We prefer the latter explanation. In either case, the original sulfur source must have had a $\delta^{34}S$ value of H_2S of at least 8.2‰. Fluid inclusion data indicate that the stage I fluid evolved mainly through dilution and cooling from boiling, possibly due to mixing of local meteoric waters into the mineralizing system. The influx of meteoric waters may be related to fracturing, as is indicated by the brecciation and multiple fracturing (and healing) of stage I veins. Therefore, we must consider influx of local meteoric waters coupled with fluid boiling to explain the systematical decrease in $\delta^{34}S_{H_2S}$ values of stage I sulfides. The assemblage hematite+sulfides (and/or sulfosalts) in the late mineralization of stage I (Fig. 2) attests to relatively oxidizing fluid conditions with a mixed, sulfate-H_2S character. The change from early to late mineralization would have resulted in increased SO_4/H_2S ratios and corresponding decreases in $\delta^{34}S$ values of H_2S (Ohmoto and Rye, 1979).

Table 2. Oxygen and hydrogen isotope data for stage I minerals from the Hwanghak mine.

Sample no.	Mineral	$\delta^{18}O$ (‰)	T(℃)[1]	$\delta^{18}O_{water}$[2] (‰)	δD_{water} (‰)
HW-1	quartz	4.4	250	−4.5	−75
HW-2	quartz	7.9	300	−1.1	−79

[1]: Based on fluid inclusion temperatures and paragenetic constraints. [2]: Calculated using the isotope fractionation equations of Matsuhisa et al. (1979).

Oxygen and Hydrogen Isotope Study

The $\delta^{18}O$ values of two quartz samples from the

Hwanghak mine are 7.9 and 4.4‰ (Table 2). Calculated $\delta^{18}O_{water}$ values, using the fractionation equation of Matsuhisa et al. (1979) coupled with fluid inclusion homogenization temperatures, are +1.1 and −4.5‰. Inclusion waters were extracted from the quartz samples. Their δD values are −79 and −75‰ (Table 2). The measured range of δD values of fluids in Cretaceous (142 to 68 Ma) Au-Ag-bearing veins in Korea is −80 to −143 per mil (Shelton et al., 1988; So and Shelton, 1987) and is assumed to represent the range of paleometeoric water compositions in Korea at the time of mineralization. Table 2 shows the measured and calculated fluid isotopic compositions of the Hwanghak mine. The range of these data is consistent with meteoric water dominance as fluid compositions approach those of local, unexchanged meteoric waters. The $\delta^{18}O$ - δD data from early and late mineralization periods in the Hwanghak deposit display various degrees of ^{18}O-enrichment (with nearly constant δD values) relative to meteoric water, produced by isotope exchange with surrounding rocks, the classic ^{18}O - shift (Taylor, 19 74). Data of the early quartz show higher ^{18}O - shift than that of the late quartz, possibly indicating relatively lower water/rock ratio for the ore fluids that deposited the early quartz. These O-H isotope data were compared to the O-H isotope values of other copper vein deposits (Keumhak, Jeonheung and Ogsan deposits, unpublished data) near the Hwanghak deposit because of insufficient data. The results show the same trends of ^{18}O - shift with increasing paragenetic time. Although we have insufficient O-H isotope data, the increasing water/rock ratios from early towards late periods of stage I mineralization are thought to indicate the influx of larger amounts of cooler, more oxidized local meteoric waters into the hydrothermal system with time.

ACKNOWLEDGEMENTS

This research was supported by Non Directed Research Fund, Korea Research Foundation, 1991. The authors acknowledge also the Center for Mineral Resources Research for partial support for field survey and stable isotope analyses.

REFERENCES

Barton, P.B.Jr. and Toulmin, P.III (1964) The electrum-tarnish method for the determination of the fugacity of sulfur in laboratory sulfides system. Geochim. Cosmochim. Acta, v. 28, p. 619-640.

Chang, K.H., Ko. I.S., Park, H.I., Chi, J.M. and Kim, H.M. (1978) Geologic sheet of Cheonji area. Korea Institute Energy Resources, 1:50,000 map.

Crerar, D.A. (1974) Solvation and deposition of chalcopyrite and chalcocite assemblages in hydrothermal solution. Ph.D. dissertation, Dept. Geological Sciences, Pennsylvania State University.

Crerar and Barnes, H.L. (1976) Ore solution chemistry V. Solubilities of chalcopyrite and chalcocite assemblages in hydrothermal solution at 200 to 350℃. Econ. Geol., v. 71, p. 772-794.

Cunningham, C.G. (1978) Pressure gradients and boiling as mechanisms for logicalizing ore in porphyry systems. Jour. Research U.S. Geol. Survey, v. 6, p. 745-754.

Ellis, A.J. and Golding, R.M. (1963) The solubility of carbon dioxide above 100℃ in water and in sodium chloride solutions. Am. Jour. Sci., v. 261, p. 47-60.

Fournier, R.O. and Truesdell, A.H. (1973) An empirical Na-K-Ca geothermometer for natural waters. Geochim. et Cosmochim. Acta, v. 37, p. 1255-1275.

Grinenko, V.A. (1962) Preparation of sulfur dioxide for isotopic analysis. Zhurnal Neorganicheskoi Khimii, v. 7, p. 2478-2483.

Hall, W.E. and Friedman, I. (1963) Composition of fluid inclusion, Cave-in-Rock fluorite district, Illinois and Upper Mississippi Valley zinc-lead district. Econ. Geol., v. 53, p. 886-911.

Hass, J.L.Jr. (1971) The effect of salinity on the maximum thermal gradient of a hydrothermal system at hydrostatic pressure. Econ. Geol., v. 66, p. 940-946.

Helgeson, H.C. (1969) Thermodynamics of hydrothermal systems at elevated temperatures and pressures. Am. Jour. Sci., v. 267, p. 729-804.

Jin, M.S., Lee, S.M., Lee, J.S. and Kim, S.J. (1982) Lithochemistry of the Cretaceous granitoids with relation to the metallic ore deposits in Southern Korea. J.Geol. Soc., Korea. v. 18, p. 119-131.

Lee, D.S. (1987) Geology of Korea. 514p, Kyohak-Sa, Seoul.

Matsuhisa, Y., Goldsmith, R. and Clayton, R.N. (1979) Oxygen isotope fractionation in the system quartz-albite-anorthite-water. Geochim. Cosmochim. Acta, v. 43, p. 1131-1140.

Matsuhisa, Y. (1986) Effect of mixing and boiling of fluids on isotopic compositions of quartz and calcite from epithermal deposits. Mining Geol. v. 36, p. 487-493.

Ohmoto, H. (1972) Systematics of sulfur and carbon isotopes in hydrothermal ore deposits. Econ. Geol., v. 67, p. 551-578.

Ohmoto, H. and Rye, R.O. (1979) Isotopes of sulfur and carbon. In Geochemistry of hydrothermal ore deposits (Barnes, H.L.Ed.) 798p, Wiley and Sons Pub. Co., New York, p. 509-567.

O'Neil, J.R. and Silberman, M.L. (1974) Stable isotope relations in epithermal Au-Ag deposits. Econ. Geol., v. 69, p. 902-909.

Park, H.I., Choi, S.W., Jang, H.W. and Chae, D.H. (1985)

Copper mineralization at Haman-Gunbuk mining district. J. Korean Inst. Mining Geol., v. 18, p. 107-124.
Potter, R.W., III, Clynne, M.A. and Brown, D.L. (1978) Freezing point depression of aqueous sodium chlolide solutions. Econ. Geol., v. 73, p. 284-285.
Romberger, S.B. and Barnes, H.L. (1970) Ore solution chemistry III. Solubility of CuS in sulfide solutions. Econ. Geol., v. 65, p. 901-919.
Scott, S.D. and Barnes, H.L. (1971) Sphalerite geothermometry and geobarometry. Econ. Geol., v. 66, p. 653-669.
Shelton, K.L. (1983) Composition and origin of ore-forming fluids in a carbonate-hosted porphyry copper and skarn deposit: A fluid inclusion and stable isotope study of Mines Gaspe, Quebec. Econ. Geol., v. 78, p. 387-421.
Shelton, K.L., So, C.S. and Chang, J.S. (1988) Gold-rich mesothermal vein deposits of the Republic of Korea: Geochemical studies of the Jungwon gold area. Econ. Geol., v. 83, p. 1221-1237.
Shepherd,T.J., Rankin,A.H. and Alderton, D.H.M. (1985) A practical guide to fluid inclusion studies. 239p, Blackie, Glasgow.
Sillitoe, R.H. (1980) Evidence for porphyry-type mineralization in Southern Korea. Mining Geol., Special Issue, v. 8, p. 205-214.
So, C.S., Chi, S.J. and Shelton, K.L. (1985) Cu-bearing hydrothermal vein deposits in the Gyeongsang Basin, Republic of Korea. Econ. Geol., v. 80, p. 43-56.
So, C.S. and Shelton, K.L. (1987) Stable isotope and fluid inclusion studies of gold- and silver-bearing hydrothermal vein deposits, Cheonan-Cheongyang-Nonsan mining district, Republic of Korea: Cheonan Area. Econ. Geol., v. 82, p. 987-1000.
Taylor, H.P.Jr. (1973) $^{18}O/^{16}O$ evidence for meteoric-hydrothermal alteration and ore deposition in Tonopah, Comstock Lode, and Goldfield mining districts, Nevada. Econ. Geol., v. 68, p. 747-764.
Taylor, H.P.Jr. (1974) The application of oxygen and hydrogen isotope studies to problems of hydrothermal alteration and ore deposition. Econ. Geol., v. 69, p. 843-883.

Manuscript received 9 July 1992

경북 옥산지역 열수동광상의 성인연구

최선규 · 최상훈 · 윤성택 · 이재호 · 소칠섭

요 약: 옥산지역에 위치하는 황학동광상은 초기백악기 퇴적암류내에 발달한 열극을 충진한 열수맥상 광상으로, 구조운동에 수반되어 3회에 걸쳐 생성된 석영 및 방해석맥으로 구성된다. 주된 금속광물로는 황철석, 자류철석, 황동석, 섬아연석, 방연석, 적철석 및 Ag-, Pb-, Bi-sulfosalts로, 이들의 침전은 주로 광화 제1기의 0.5~7.6 wt.% NaCl 상당염농도를 갖는 광화유체로부터 370℃에서 약 200℃에 걸쳐 진행되었으며, 광화 작용시의 압력은 <180 bar, 심도는 700~2,400 m 였다. 광상내에서 보여주는 광물공생관계에 의한 열역학적 고찰과 유체포유물 및 안정동위원소 연구결과 등으로 미루어 본 광상광화유체내 Cu는 주로 chloride complex 상으로 이동되었으며, 주로 광화유체의 냉각작용과 이에 의한 지화학적 환경요인들(fs_2, fo_2, pH)의 변화에 기인하여 침전되었음을 알수 있다. 유황안정동위원소 연구결과, 주광화시기인 광화1기중 광화유체의 $\delta^{34}S_{H_2S}$ 값이 초기 8.2‰에서 후기 4.7‰로 점차 감소함은 광화유체의 비등에 수반되어 수소이온농도와 함께 산소분압이 점진적으로 증가한 결과로 해석되며, 광화유체의 수소 및 산소동위원소 값으로부터 열수계에서 천수가 지배적인 역할을 하였음을 알수 있다.